BMC Cancer

RESEARCH

Open Access

Deciphering the anti-neoplastic potential of *Allium ascalonicum* in averting the proliferation and epithelial-mesenchymal transition of triple-negative breast cancer through virtual docking and In Vitro approaches

Karunya Jenin Ravindranath[1] and Hemalatha Srinivasan[1*]

Abstract

Background Universally, *Allium ascalonicum* (Shallots) is a well-known flavouring agent in many cuisines. Though, it's been proved for its health benefits due to the presence of alkaloids, flavonoids, terpenoids, phenols and coumarins, its role as an anti-neoplastic agent still requires comprehensive investigation. In our study, we have investigated the presence of potential anti-neoplastic phytocompounds, anti-inflammatory, cytotoxicity and anti-metastatic activity of Shallots against Triple-Negative Breast Cancer cell line, MDA-MB-231.

Methods Phytocompounds of aqueous *Allium ascalonicum* extract (AAE) derived from GC–MS and LC–MS analysis were docked with an inflammatory marker, Interleukin-18 (IL-18); anti-apoptotic proteins, B-cell Lymphoma-2 (BCL-2) and Myeloid Cell Leukemia-1 (MCL-1); and metastatic marker, Vimentin using PyRx (Version 0.9.9). Subsequently, the anti-inflammatory property of AAE was determined using Bovine Serum Albumin (BSA) Denaturation Assay and the chemotherapeutic potential of AAE was determined using 3-(4,5-Dimethylthiazol-2-yl)-2,5-Diphenyltetrazolium Bromide (MTT) assay on MDA-MB-231 and HEK293T cell lines. Additionally, to determine the synergistic effect of Doxorubicin Hydrochloride (Standard) and AAE, MTT assay was performed on MDA-MB-231 cell lines treated with the combination therapy. Furthermore, the anti-metastatic property of AAE was determined using cell migration and clonogenic assays. Finally, Dual Acridine Orange/Ethidium Bromide fluorescence staining method was used to determine if AAE has the ability to induce apoptosis and necrosis in MDA-MB-231 cells.

Results Molecular docking results using the compounds obtained from LC–MS and GC–MS with the target proteins revealed promising anti-neoplastic bioactive compounds. BSA Denaturation assay proved that AAE has anti-inflammatory property, with the highest, 85.78% observed at 2 mg/ml of AAE. Moreover, MTT assay proved that AAE exhibited cytotoxic effect on MDA-MB-231 in a dose-dependent manner, with an IC_{50} observed at 1.23 mg/ml (**$p \leq 0.005$) and non-toxic to HEK293T cells. Combination therapy of the standard with AAE reduced the IC_{50} of the standard by 65.5%. Consecutively, the anti-metastatic property of AAE was proved using cell migration and clonogenic assays, suggesting suppression of epithelial-mesenchymal transition. Finally, Dual Acridine Orange/Ethidium Bromide fluorescence staining method displayed that, AAE has the ability to induce apoptosis and necrosis in TNBC cells.

*Correspondence:
Hemalatha Srinivasan
hemalatha.sls@bsauniv.ac.in

Conclusion The outcomes from in vitro assays corroborated with the molecular docking results and hence, on authenticating the potentiality of AAE's anti-neoplastic effect via. in vivo models, pre-clinical and clinical trials, *Allium ascalonicum* can be articulated to a prospective anti-neoplastic drug for treating TNBC.

Keywords *Allium ascalonicum*, Molecular Docking, Anti-inflammatory, TNBC, Chemotherapeutic, Anti-metastatic

Graphical Abstract

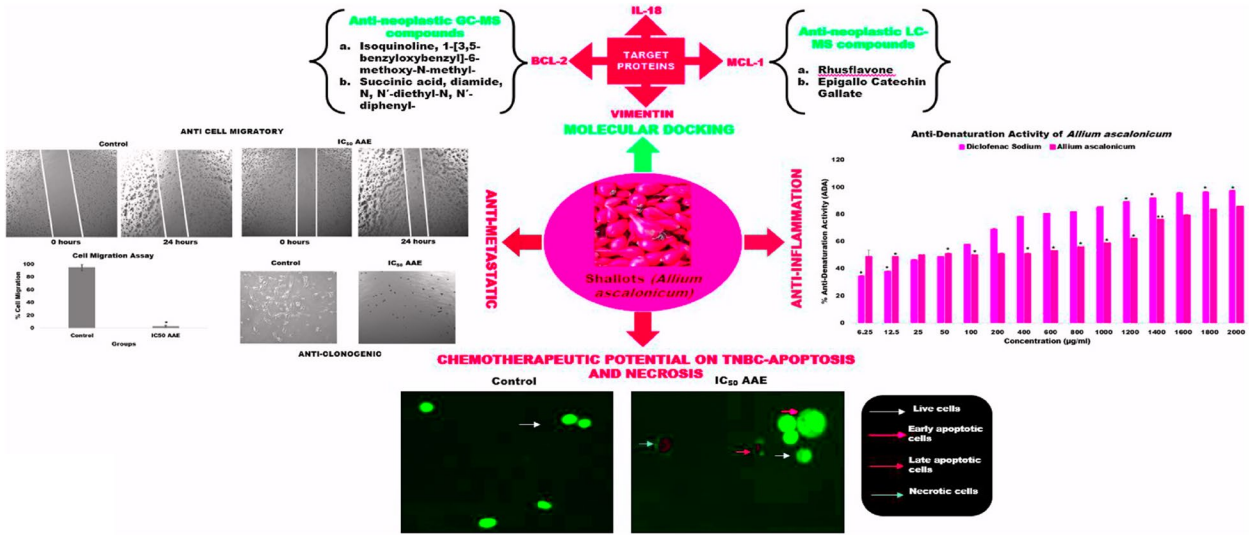

Introduction

TNBC is a miscellaneous disease with varied clinical and biological characteristics, commonly reported to be occurring in younger women and women with BRCA1 gene mutation. Moreover, TNBC accounts for nearly 15% of the newly diagnosed neoplasms of the breast [1] and several gene-expression-based TNBC classifications were developed during the past few decades [2, 3]. The five-year survival rate of TNBC was reported to be 77%, contrary to the 93% observed in the other breast cancer sub-types, as per the statistical report based on 2012–2018 cases by the American Cancer Society [4]. The absence of broad-spectrum therapeutic agents for TNBC due to the deficiency in the expression of HER2 and targetable hormonal receptors, progesterone and estrogen, in addition to the poor prognosis has enthralled breast cancer researchers [5]. Precisely, TNBC is functionally defined, as an array with varied clinical and biological behavior with specific differences in histology, transcription and genetics among breast cancer cases [6]. Due to the heterogenous nature of the disease, nominating a particular treatment option based on the carcinoma profile of the breast neoplasm patients is quite complicated.

Commonly used treatment preferences to manage the severity of TNBC include, using taxanes for p53 mutated tumors, targeting DNA repair complex using platinum compounds and taxanes, tumor cell proliferation with the help of anthracyclines and many more targeted approaches [7]. Chemotherapeutic drug, tamoxifen, has reports of enhancing uterine cancer and thromboembolism [8]. Distinguishable side-effects of chemotherapy observed in patients with breast neoplasms include, loss of appetite, fatigue, nausea and vomiting, anemia, muscle/joint pain, sleep disorders, alopecia (due to anthracyclines) etc. [9]. Similarly, radiation therapy has its own toxic side-effects, namely, edema, skin changes, tenderness, fatigue, hair loss etc. [10]. Hence, there is a crucial need for the development of novel drugs from the bioactive components of the plant-based resources that are efficacious and safe.

In this study, Shallots (*Allium ascalonicum*) belonging to the group, *Allium* vegetables was extensively researched to determine its cytotoxic activity against TNBC. Since traditional times, Shallots have been broadly used as herbal supplements [11]. Referred as bulb crops and are used as special culinary ingredients, because of their distinct aroma generated (from organic sulfur compounds) during the enzymatic degradation of the precursors (S-alk(en)yl cysteine sulfoxide), present in the cells (by allinase and lachrymatory factor synthase).

This breakdown releases sulfur compounds and other bioactive substances (flavonols and other phenols) that have the ability to prevent and treat a variety of human illnesses, including microbial infections, cancer and degenerative disorders [12]. The anti-microbial, anti-protozoal, antioxidant and anti-inflammatory properties of Shallots have also been well studied and proved [12]. Anti-carcinogenic activity of aqueous shallot extracts has been demonstrated in liver cancer cell lines (HepG2) [13], K562 and Jurkat cell lines [14] and also in breast cancer cell lines (MCF-7) [15] with significant cytotoxic effects. However, its cytotoxic activity against TNBC is not yet established and hence in this research work, we have attempted to determine the anti-neoplastic potential of *Allium ascalonicum* in TNBC.

Primarily, in our current research work, the presence of anti-neoplastic phytocompounds in *Allium ascalonicum* was studied using Gas chromatography-Mass spectrometry (GC–MS) [15] and Liquid chromatography-Mass spectrometry (LC–MS). These phytocompounds and a standard anti-neoplastic drug, Gemcitabine, were docked with IL-18 (an inflammatory cytokine), BCL-2 and MCL-1 (anti-apoptotic proteins involved in TNBC malignancy) and Vimentin (a metastatic marker) for the identification of influential anti-neoplastic phytocompounds in treating TNBC through in silico approaches. In our previous research work published [15], we had already proved that the aqueous extract of *Allium ascalonicum* is effective against breast cancer cell line, MCF-7. Hence, in our current research study, we had extended our work further and therefore, the lyophilized sample of aqueous extract of *Allium ascalonicum* was analyzed for the determination of anti-inflammatory activity, cytotoxic effect and anti-metastatic activity (cell migration and clonogenic assays) on TNBC cell line, MDA-MB-231 based on the hypothesis that *Allium ascalonicum* possess anti-neoplastic activity against TNBC.

Materials and methods

Preparation of *Allium ascalonicum* Extract (AAE)

The bulbs of *Allium ascalonicum* were thoroughly washed to remove the unwanted dirt and sand. The bulbs were crushed well and then grinded using double distilled water. The grounded contents were then filtered using Whatman No. 1 Filter paper and then freeze-dried using lyophilizer (Martin Christ Alpha 2–4 LD Plus Freeze-Dryer, Germany). The freeze-dried AAE was then used for subsequent in vitro assays.

Gas-chromatography mass spectrometry analysis of *Allium ascalonicum*

GC–MS apparatus (Shimadzu Corporation, Kyoto, Japan) was used for characterization of phytocompounds in *Allium ascalonicum,* as reported by Mir and Bashir et al., 2020 [16]. The capillary column with an inner diameter of 15 m length x 250 µm, coated with a 0.25 µm film thickness stationary phase (Rtx-5MS, Restek corporation, Bellefoente PA, USA) was used for segregating the plant sample components. The gas carrier used was 99.99% Helium, with the linear velocity of 36.2 cm/sec. An autoinjector was used to inject 2 µl of the plant sample on splitless mode at 300°C. Initially, the GC oven was programmed at 60°C for 1 min and then heated at 40°C/min, until 300°C and held for 10 min with an equilibration time set to 0.5 min. The pressure and the flow rate were set to 9.3508psi and 1 mL/min to 1.2 mL/min respectively. The peak compounds were identified using the total ion chromatogram (TIC) obtained after analysis along with the corresponding peak area. National Institute of Standards and Technology (NIST) database was used for comparing and identifying peak compounds in GC mass spectra. The number of counts for each component per unit time (mins) obtained during GC operation was used to estimate the area of the peak compounds.

Liquid-chromatography mass spectrometric analysis of *Allium ascalonicum*

A sophisticated analytical instrument, Xevo G2-XS QTof, Waters, USA with a 1525 microns Binary pump was used for performing LC–MS analysis of *Allium ascalonicum*. The column packed with Accucore C18, 50 × 4.6 mm, 5micron particle size (Thermo Scientific) was used with 0.1% Formic acid in water as mobile phase-A, Acetonitrile as mobile phase-B at a flow rate of 0.5 ml/min. Gradient elution analysis was performed and represented as (Time-A/B): 0 min-95/5, 1 min-95/5, 8 min-50/50, 12 min-5/95, 17 min-5/95, 18 min-95/5 and 20 min-95/5. Further parameters include, the capillary voltage at 3 kV; Collision Energy at 20 V; Ramp Collision Energy at 30–90 V; Source Temperature 150°C; Desolvation Temperature 450°C; Cone gas 50L/hr; Desolvation Gas Flow 800L/hr and the processing software was MassLynxV4.1 [17]. Nearly, 10 µl of the methanolic extract of *Allium ascalonicum* was filtered and injected. On the basis of the retention time and mass spectra, the phytocompounds of *Allium ascalonicum* were identified. Time-of-flight analyzers and hybrid quadruple [17] were used for both positive mode and negative mode mass spectral analysis (Additional File 1, Figures S1 and S2). Vaniya/Fiehn Natural product library (University of California, Davis, US) MS m/z database was used to analyze the elemental composition of ions, to facilitate the recognition of the phytocompounds present in the *Allium ascalonicum* extract (Additional File 1, Table S1).

Virtual docking analysis

A comprehensive literature survey of the list of phytocompounds obtained from GC–MS [15] and LC–MS (Additional File 1, Figures S4 and S5, Table S1) was performed initially and then, the compounds were selected based on the anti-carcinogenic properties reported in the literature. The selected compounds were then screened for ADME properties using SwissADME (http://www.swissadme.ch/) and only those compounds that obeyed Lipinski's Rule of Five were considered for molecular docking studies (Additional File 1, Table S2). Anti-neoplastic compounds obtained from the mass spectrometric analysis of *Allium ascalonicum* were docked with the target proteins, IL-18, BCL-2, MCL-1 and Vimentin (Additional File 1, Figure S3) whose Protein Data Bank (PDB) IDs are 3WO4, 4AQ3, 5FDR and 3KLT respectively. The holographic structure of the target proteins and that of the anti-neoplastic compounds were obtained from PDB database (https://www.rcsb.org/) and PubChem (https://pubchem.ncbi.nlm.nih.gov/) correspondingly. It was then proceeded further, for docking analysis using a multi-ligand docking program named, PyRx (Version 0.9.9) [18]. The holographic and two-dimensional representative images were visualized using BIOVIA Discovery Studio Visualizer 2021.

Bovine serum albumin denaturation assay

Anti-inflammatory activity of AAE was determined using protocol described by Kola et al., 2022 [19] with slight modifications. Experiment was performed as triplicates in a 96-well plate using varying concentrations of AAE and the standard (Diclofenac Sodium) ranging from 6.25 µg/ml to 2000 µg/ml and then treated with 0.2% of BSA dissolved in Tris-Buffered Saline (TBS) at pH 6.8. The standard drug treated with 0.2% of BSA served as a positive control. The 96-well plate was then kept for incubation at 37 °C and 72 °C for 15 min and 5 min respectively. The plate appearing turbid was then read using a multimode plate reader (PerkinElmer EnSpire, USA) at 660 nm to determine the % Anti-Denaturation Activity of AAE using the equation below,

$$\%\ Anti-Denaturation\ Activity = \left[\frac{A.PC - A.AAE}{A.PC}\right] \times 100\%$$

where, A. PC = Positive Control (Absorbance) and
A. AAE = *Allium ascalonicum* extract (Absorbance)

Cytotoxicity analysis of AAE, Doxorubicin Hydrochloride and combination of IC_{50} dose of AAE with Doxorubicin Hydrochloride on MDA-MB-231 cell line

Protocol described in our previous research work, Ravindranath et al., 2023 [15] was followed, in order to determine the cytotoxic impact of AAE on MDA-MB-231 (TNBC) and HEK293T (Human Embryonic Kidney) cell lines purchased from National Centre for Cell Science, Pune, India. DMEM complete media was used to culture the cell lines in a humidified incubator chamber supplied with 5% CO_2 at 37°C. The cytotoxicity experiment was performed in triplicates with the MDA-MB-231 cells treated with different concentrations of AAE (varying from 0 µg/ml to 2000 µg/ml) and HEK293T cells (varying from 0 µg/ml to 1400 µg/ml), using a 96-well tissue culture plate. MTT at 0.5 mg/ml was added and DMSO was used to solubilize the purple formazan crystals. The absorbance values were read using a multi-mode plate reader (PerkinElmer EnSpire, USA) at test wavelength of 570 nm and reference wavelength of 620 nm for the determination of % Viability of MDA-MB-231 cells and HEK293T cells using the equation below,

$$\%Viability\ of\ MDA-MB-231\ and\ HEK293T\ cells = \left(\frac{A.AAE}{A.Control}\right) \times 100\%$$

where, A. AAE = Absorbance of *Allium ascalonicum* extract and
A. Control = Absorbance of Control

MTT assay was also performed by treating TNBC cells with Doxorubicin Hydrochloride standalone ranging from 0 µg/ml to 10 µg/ml to determine its IC_{50}. Subsequently, combination treatment with IC_{50} concentration of AAE with different concentrations of Doxorubicin Hydrochloride (0, 0.01, 0.05, 0.1, 0.25, 0.5 and 1 µg/ml), was used to treat TNBC cells in order to determine its cytotoxicity and reduction in the dosage of IC_{50} of Doxorubicin Hydrochloride using MTT procedure as described above. $IC_{50,}$ the half maximal inhibitory concentration was also estimated for all types of treatment using a linear regression plot through extrapolation.

Cell migration assay

The anti-metastatic activity was determined by the ability of AAE (IC_{50}) treated MDA-MB-231 cells to migrate into the fabricated wounds created in tissue culture plates, referred as cell migration or wound healing assay. The protocol by Park et al., 2013 [20] for cell migration assay was followed with least modifications. MDA-MB-231 cells were seeded in a 6 well plate at a density of 0.3×10^6 cells/well and then allowed for adherence and proliferation for 24 h in a humidified, 5% CO_2 incubator at 37°C.

On observing 80% confluency, a scratch was artificially created using a sterile microtip. The cell remains were then discarded using PBS and treated with AAE at IC_{50} concentration for another 24 h. Cells unexposed to treatment were considered as control. Cell fixation was performed using 75% methanol and further washed with cold PBS. Images of the injured section and area of cell migration were taken at 0 h and 24 h respectively using microscope (Carl Zeiss Axio Vert. A1, Germany). The images were then analysed using the ImageJ software to measure the width of the scratch at 0 h and 24 h in both the control and the IC50 AAE treated group of MDA-MB-231 cells. The percentage of cell migration was evaluated using the formula,

$$\%\ Cell\ migration = \frac{SA\ 0\ hrs - SA\ 24hrs}{SA\ 0\ hrs} \times 100\%$$

where, SA 0 hrs = Scratch Area at 0 hours and
SA 24 hrs = Scratch Area after 24 hrs

Clonogenic assay

The anti-metastatic activity of AAE can also be confirmed by culturing minimum number of IC_{50} treated MDA-MB-231 cells in a fresh tissue culture plate with DMEM complete media, to observe if AAE could inhibit the proliferation as well as its ability to form clones. The potential of individual MDA-MB-231 cells to maintain its capability to proliferate and expand into a colony was assessed using Clonogenic assay as described by Rafehi et al., 2011 [21] and Fazeela et al., 2018 [22]. 0.3×10^6 cells were seeded in a single well of a 6-well plate and on attaining confluency, TNBC cells were treated with AAE at IC_{50} concentration and the untreated cells were used as control. After 24 h, the cells were trypsinized to obtain individual cell suspension. 500 cells from the cell suspension were seeded onto a fresh plate and were then left undisturbed for a week. DMEM complete media was then discarded and cleansed using PBS and fixed with ice-cold 70% Methanol at 4°C for 10–15 min. Trypan blue was then added to visualize the colony formation/non-formation of MDA-MB-231 cells using Carl Zeiss Axio Vert. A1 microscope, Germany.

Dual acridine orange/ Ethidium Bromide (AO/EtBr) fluorescent staining assay

In brief, TNBC cells were seeded at a density of 0.3×10^6 cells per well in a 6 well plate. On achieving 70%—80% confluency, the cells were treated with IC_{50} of AAE for 24 h and the untreated cells were used as control. The dual AO/EtBr fluorescent staining assay was performed as per the protocol described by Liu et al., 2015 [23] and Kepekçi et al., 2021 [24]. The untreated and the treated cells were then trypsinized and 25 µl of cell suspensions were transferred on to the glass slides. 1 µl of the equally mixed, 100 µg/ml AO and 100 µg/ml of EtBr was added on to the suspended cells in the glass slides, mixed well and then covered with a cover slip. The various stages of apoptosis and necrotic TNBC cells were observed under the fluorescence microscope (Carl Zeiss Axio Vert. A1, Germany), within a maximum time period of 20 min, after addition of the dye. The percentage rate of apoptotic cells was determined using the quantity of cells observed within the microscopic range of both the control and IC_{50} AAE treated cells.

Data interpretation and validation

Experimental data obtained, mean ± standard deviation was interpreted statistically and validated using Student's T-test using Microsoft Excel program with probability values, ≤ 0.05, ≤ 0.005 and ≤ 0.001 represented as $^{*}p$ (statistically significant), $^{**}p$ (high statistical significance) and $\#p$ (highest statistical significance) respectively.

Results

Recognition of potential anti-neoplastic phytocompounds

Molecular docking of anti-neoplastic phytocompounds with target proteins, IL-18, BCL-2, MCL-1 and Vimentin helped us to recognize potential anti-neoplastic phytocompounds that could be playing a significant role in inhibiting the progression of TNBC. Basically, ligands exhibiting binding affinity values ≤ −6.0 kcal/mol are considered best [15] and hence the phytocompounds with binding affinity values lower than that of the standard drug, Gemcitabine were identified and tabulated along with the interacting aminoacid residues (Table 1 and Table 2). Gemcitabine kills breast cancer cells; however, it is also known to cause definite side-effects, namely, enhanced risk of infection, breathlessness, bruising, nosebleeds, feeling sick, abnormal liver changes, flu, hair loss, fatigue, skin rash, blood and protein in urine, etc. [25]. These side-effects were prone to affect everyday lives of afflicted patients majorly. Hence, this drug has been used as a standard ligand in docking analysis for comparative studies on binding association values of anti-neoplastic phytocompounds of *Allium ascalonicum*. On comparing the binding affinity values of Gemcitabine with the anti-neoplastic compounds of AAE, we could infer that, the phytocompounds of AAE interact with the target receptors and form more stable interactions when compared to the standard and, thereby, validating significant anti-neoplastic potential of AAE.

According to the molecular docking results of GC–MS compounds (Table 1), the phytocompound, Isoquinoline, 1-[3,5-benzyloxybenzyl]−6-methoxy-N-methyl- has the best binding affinity values of −8.1, −8.7, −9.3 and

Table 1 Identification of potential GC–MS anti-neoplastic compounds of *Allium ascalonicum* based on binding affinity values and the list of amino acid residues present in the target proteins that interact with them

Target Proteins	Ligands	Amino acid residues involved	Binding Affinity (Kcal/mol)
IL-18 (Interleukin-18)	**Gemcitabine** a) Isoquinoline, 1-[3,5-benzyloxybenzyl]−6-methoxy-N-methyl- b) Succinic acid, diamide, N, N′-diethyl-N, N′-diphenyl-	**Chain A: LYS112, *HIS109*, GLY108;** **Chain B: *ARG210*, *LYS134*, LYS128;** **Chain C: GLU210** Chain B: GLY274, ASP209, GLU244; Chain C: LYS313, THR 247, LEU 249 Chain A: *HIS109*; Chain B: *LYS134*, *ARG210*, ILE129	**−7.0** −8.1 −7.6
BCL-2 (B-Cell Lymphoma-2)	**Gemcitabine** a) Isoquinoline, 1-[3,5-benzyloxybenzyl]−6-methoxy-N-methyl- b) Succinic acid, diamide, N, N′-diethyl-N, N′-diphenyl-	**Chain B: *PHE71*, SER64, ARG68, VAL115, GLU111** Chain B: VAL92, ASN102, PHE63, ARG105, ALA108, LEU96, TYR67, MET74, *PHE71* Chain B: PHE89, ALA90	**−6.3** −8.7 −6.5
MCL-1 (Myeloid Cell Leukemia-1)	**Gemcitabine** a) Isoquinoline, 1-[3,5-benzyloxybenzyl]−6-methoxy-N-methyl- b) Succinic acid, diamide, N, N′-diethyl-N, N′-diphenyl- c) 2-Amino-4-phenylpyrimidine d) Pyrrole, 2-methyl-5-phenyl- e) 6-Indolizinecarbonitrile,2-methyl-	**Chain D: *MET250*, *PHE270*** Chain C: ARG263, VAL274, PHE270, MET250, LEU246, LEU267, VAL253 Chain B: ALA227, LEU235, LEU246, PHE270, VAL249, MET250, VAL253, LEU267, MET231 Chain D: VAL253, LEU267, *PHE270*, VAL249, *MET250* Chain B: LEU235, MET250, LEU246, VAL249, VAL253, PHE270, LEU267 Chain D: LEU267, *PHE270*, LEU235, LEU246, VAL249, *MET250*	**−6.5** −9.3 −8.3 −7.2 −7.2 -6.8
Vimentin	**Gemcitabine** a) Isoquinoline, 1-[3,5-benzyloxybenzyl]−6-methoxy-N-methyl- b) Pyrrole, 2-methyl-5-phenyl- c) 2-Amino-4-phenylpyrimidine d) Succinic acid, diamide, N, N′-diethyl-N, N′-diphenyl- e) 6-Indolizinecarbonitrile, 2-methyl f) N-(4-Bromomethylphenyl)acetamide	**Chain D: *TYR276, ARG 273*** Chain A: ASN283, VAL279, ALA280; Chain B: TYR276, ALA280, LEU284, VAL279; Chain C: TRP290, TYR291, LEU284; Chain D: TYR291, GLU286, ALA287, TRP290 Chain A: TYR291, PHE295; Chain D: *ARG273, TYR276* Chain A: TYR291; Chain B: TYR291; TYR276 Chain A: VAL279; Chain B: VAL279; Chain C: ALA287, TRP290, TYR291; Chain D: TYR291, ALA287 Chain A: PHE295; Chain D: *TYR276, ARG273* Chain A: TYR291; Chain B: TYR291; Chain C: TYR276, VAL272; Chain D: *TYR276, ARG273*	**−6.7** −10.1 −8.0 −7.8 −7.4 −7.2 −7.0

* *Italicized amino acid residues gives information about the similar residue interactions between the standard and the potential anti-neoplastic compounds*

LYS Lysine, *HIS* Histidine, *GLY* Glycine, *ARG* Arginine, *GLU* Glutamic acid, *GLY* Glycine, *ASP* Aspartic acid, *THR* Threonine, *LEU* Leucine, *ILE* Isoleucine, *PHE* Phenylalanine, *SER* Serine, *VAL* Valine, *ASN* Asparagine, *ALA* Alanine, *TYR* Tyrosine, *MET* Methionine, *TRP* Tryptophan

−10.1 kcal/mol with all the four target proteins, IL-18, BCL-2, MCL-1 and Vimentin respectively when compared to the standard, Gemcitabine. Succinic acid, diamide, N, N′-diethyl-N, N′-diphenyl- demonstrated as the second best phytocompound during its interaction with IL-18, BCL-2 and MCL-1, whereas, Pyrrole, 2-methyl-5-phenyl- displayed as the second best phytocompound for Vimentin.

In accordance with the molecular docking results of LC–MS compounds (Table 2), the phytocompound, Rhusflavone proved to be the best in terms of binding affinity scores, −9, −8.3 and −11 kcal/mol for the target proteins, IL-18, BCL-2 and Vimentin respectively. The second best phytocompound observed was Epigallo Catechin Gallate with binding affinity scores of −8.3, −6.8, −9.4 and −8.4 kcal/mol for IL-18, BCL-2, MCL-1 and Vimentin respectively. The best compounds were selected based on comparison of the binding affinity values of the phytocompounds with that of the standard, Gemcitabine. The 3D holographic images of the

Table 2 Identification of potential LC–MS anti-neoplastic compounds of *Allium ascalonicum* based on binding affinity values and the list of amino acid residues present in the target proteins that interact with them

Target Proteins	Ligands	Amino acid residues involved	Binding Affinity (Kcal/mol)
IL-18 (Interleukin-18)	**Gemcitabine**	**Chain A: *LYS112*, HIS109, *GLY108*;**	**−7.0**
	a) Rhusflavone	**Chain B: *ARG210*, *LYS134*, *LYS128*;**	−9.0
	b) Myricitrin	**Chain C: *GLU210***	−8.4
	c) Epigallo Catechin Gallate	Chain B: GLU208, *ARG210*, GLU243,	−8.3
	d) Phylloquinone	GLU244, GLY274; Chain C: LYS248	−7.7
	e) Obtusinin	Chain C: SER158, ARG37, GLN150,	−7.5
	f) Pantoyl Lactone Glucoside	ASN152, ALA153, GLU40, ALA159	−7.3
	g) Trehalose	Chain C: SER158, ALA153, SER179,	−7.2
		CYS180, SER177, SER35, GLU40, ARG37	
		Chain A: *LYS112*; Chain B: *LYS134*,	
		ARG210, GLU131, *LYS128*, ILE129	
		Chain A: *LYS112*, *GLY108*, ASN111;	
		Chain B: *LYS128*, *ARG210*, GLU131	
		Chain A: *LYS112*, *GLY108*; Chain B:	
		ARG210, GLU131, *LYS134*;	
		Chain C: *GLU210*	
		Chain A: *LYS112*, ASN111;	
		Chain B: GLU131, PHE135, ILE129; Chain C: *GLU210*, GLY168	
BCL-2 (B-Cell Lymphoma-2)	**Gemcitabine**	**Chain B: PHE71, SER64, *ARG68*,**	**−6.3**
	a) Rhusflavone	***VAL115*, GLU111**	-8.3
	b) Phylloquinone	Chain A: ARG98, PHE89, TYR130,	−7.3
	c) Epigallo Catechin Gallate	VAL93, ALA90	−6.8
	d) Myricitrin	Chain A: ARG98, HIS143, ARG142,	−6.8
	e) Obtusinin	TYR139, VAL93, ALA90, TRP135,	−6.3
		PHE89, ARG86	
		Chain A: ARG86, GLU138, TRP135,	
		PHE89	
		Chain B: *VAL115*, *ARG68*, SER75, ASN122, GLU119, ARG26, VAL118	
		Chain B: ARG26, *VAL115*, GLU119,	
		VAL118, *ARG68*, LYS22	
MCL-1 (Myeloid Cell Leukemia-1)	**Gemcitabine**	**Chain D: MET250, PHE270**	**−6.5**
	a) Epigallo Catechin Gallate	Chain B: ALA227, VAL253, MET250,	−9.4
	b) Rhusflavone	PHE270	−9.1
	c) Phylloquinone	Chain C: PHE270, MET250, LEU267,	−8.1
	d) Myricitrin	ARG263, VAL253, THR266	−7.5
	e) Obtusinin	Chain A: ARG222, ASN223; Chain B:	−7.4
	f) Trehalose	PHE270, LEU267, VAL253, HIS224	−6.8
		Chain B: SER293, GLU292, LYS244;	
		Chain C: SER245, ASP236, LEU235	
		Chain C: PHE270, GLY271, LEU246,	
		VAL274, VAL249, MET250, VAL253,	
		MET231	
		Chain A: GLU225, THR226, ARG222;	
		Chain B: ASP256; Chain C: HIS252	
Vimentin	**Gemcitabine**	**Chain D: *TYR276*, *ARG 273***	**−6.7**
	a) Rhusflavone	Chain A: ALA287, TYR291, GLU288;	−11.0
	b) Epigallo Catechin Gallate	Chain B: ASN283, TYR291, ALA287;	−8.4
	c) Phylloquinone	Chain C: ALA280; Chain D: ALA280, *TYR276*	−7.8
	d) Myricitrin	Chain A: ASN283, ALA280; Chain C:	−7.7
	e) Obtusinin	TYR 291, ALA287, GLU286	−7.0
	f) Cinnamic acid	Chain A: ASN283, ALA280, VAL279;	−6.7
		Chain B: VAL279, TYR276; Chain C:	
		TYR291, ALA287, TRP290;	
		Chain D: TYR291	
		Chain B: TYR291, ALA287, ASN283,	
		LEU284; Chain D: VAL279	
		Chain B: VAL279, TYR276;	
		Chain D: GLU286, ALA287, TRP290,	
		TYR291, ASN282	
		Chain D: *ARG273, TYR276*	

[*] *Italicized amino acid residues gives information about the similar residue interactions between the standard and the potential anti-neoplastic compounds*

LYS Lysine, *HIS* Histidine, *GLY* Glycine, *ARG* Arginine, *GLU* Glutamic acid, *GLY* Glycine, *ASP* Aspartic acid, *THR* Threonine, *LEU* Leucine, *ILE* Isoleucine, *PHE* Phenylalanine, *SER* Serine, *VAL* Valine, *ASN* Asparagine, *ALA* Alanine, *TYR* Tyrosine, *MET* Methionine, *TRP* Tryptophan

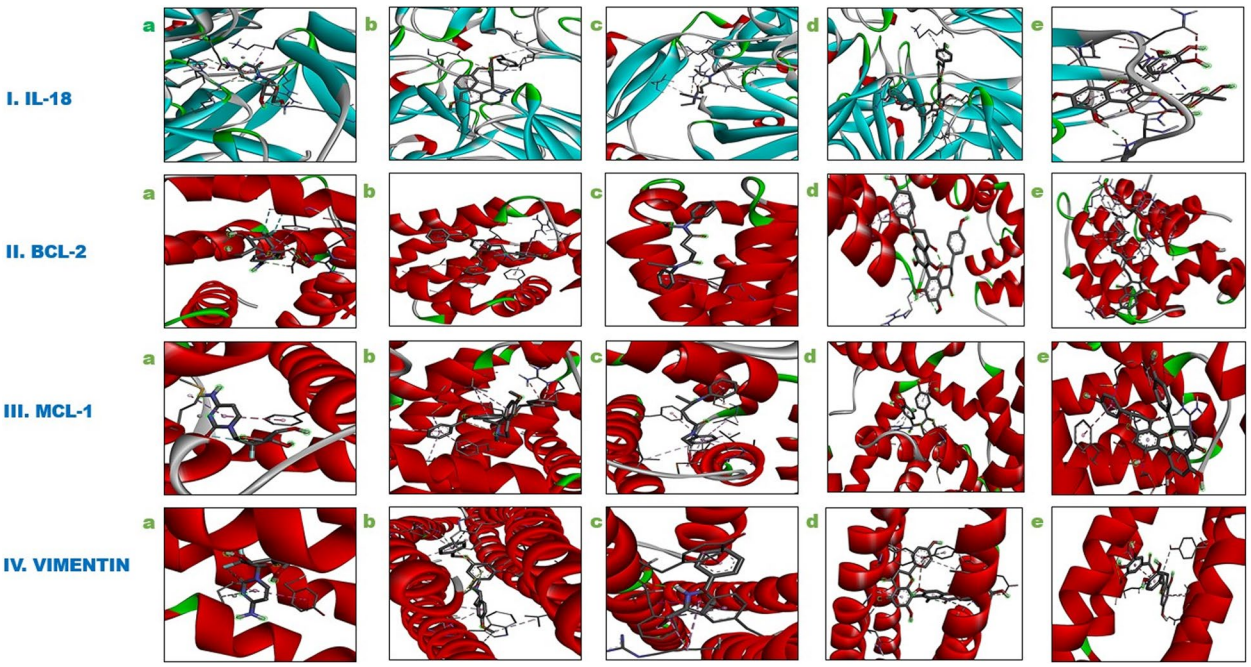

Fig. 1 Holographic interaction images of target proteins with standard and best phytocompounds from GC–MS and LC–MS. I. IL-18 (Interleukin-18) with a. Gemcitabine b. Isoquinoline, 1-[3,5-benzyloxybenzyl]–6-methoxy-N-methyl- c. Succinic acid, diamide, N, N′-diethyl-N, N′-diphenyl- d. Rhusflavone e. Myricitrin II. BCL-2 (B-Cell Lymphoma-2) with a. Gemcitabine b. Isoquinoline, 1-[3,5-benzyloxybenzyl]–6-methoxy-N-methyl- c. Succinic acid, diamide, N, N′-diethyl-N, N′-diphenyl- d. Rhusflavone e. Phylloquinone III. MCL-1 (Myeloid Cell Leukemia-1) with a. Gemcitabine b. Isoquinoline, 1-[3,5-benzyloxybenzyl]–6-methoxy-N-methyl- c. Succinic acid, diamide, N, N′-diethyl-N, N′-diphenyl- d. Epigallo Catechin Gallate e. Rhusflavone IV. Vimentin with a. Gemcitabine b. Isoquinoline, 1-[3,5-benzyloxybenzyl]–6-methoxy-N-methyl- c. Pyrrole, 2-methyl-5-phenyl- d. Rhusflavone e. Epigallo Catechin Gallate

interactions of the best phytocompounds (GC–MS and LC–MS) with the standard and the target proteins were represented (Fig. 1).

Additionally, Tables 1 and 2 provide information about the amino acid residues that interact between the target proteins and the ligands. It was also observed that, there are similar interacting amino acid residues for both the standard drug and the ligands with the target proteins. However, the ligands interact with a much lower binding affinity value when compared to the standard drug, hence, confirming more stable interactions of phytocompounds of AAE with the target proteins, thus, emphasizing the presence of potential therapeutic phytocompounds in AAE.

AAE exhibits anti-inflammatory potential

The anti-inflammatory capability of AAE was examined by observing its ability to prevent the denaturation of BSA at different concentrations. The anti-denaturation activity of AAE was higher, when compared to the standard, Diclofenac Sodium at lower concentrations from 6.25 µg/ml to 50 µg/ml, whereas, from 100 µg/ml till 2000 µg/ml, the standard dominated the anti-denaturation activity. The highest anti-denaturation activity of AAE, 85.78% was observed at 2000 µg/ml, whereas, the standard exhibited 97.53% at the same concentration, confirming the dose-dependent response curves for both standard and AAE, as represented in Fig. 2. The assay also proves the fact that AAE possess significant anti-inflammatory potential.

AAE induced chemotherapeutic effect on MDA-MB-231 cells and not on HEK293T cells

The graph (Fig. 3a), clearly demonstrates, that as the concentration of AAE increases, the percentage viability of the MDA-MB-231 cells decreases in a dose-proportional fashion, validating the fact that AAE has inherent capability to induce apoptosis of TNBC cells. Moreover, the half-maximal inhibitory concentration of AAE (IC_{50}) was estimated using the straight-line equation of the linear regression curve along with R^2, that is, correlation coefficient. The IC_{50} of AAE was obtained at 1.23 mg/ml ($^{**}p \leq 0.005$) and R^2 was 0.84 (Fig. 3b), indicating the presence of very good correlation between the percentage viability of TNBC cells and concentration of AAE. HEK293T cells exhibited 77% viability at 1.2 mg/ml of AAE (Fig. 3c) proving the fact that AAE is not as toxic to normal Human Embryonic Kidney cell lines when

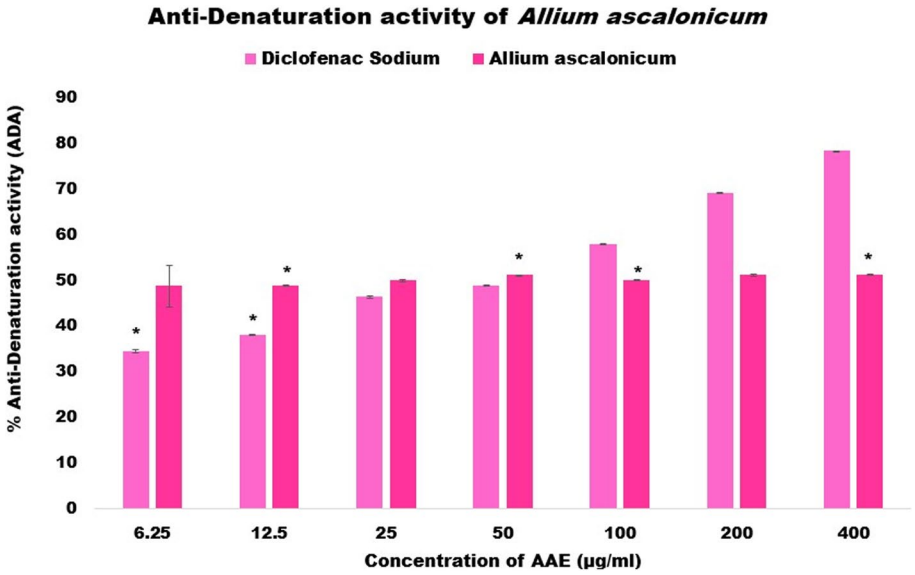

Fig. 2 Anti-Denaturation activity of *Allium ascalnonicum* using BSA Denaturation Assay. *$p \leq 0.05$ denotes statistical significance and **$p \leq 0.005$ represents high statistical significance of the experiment with the positive control group and error bar in the graphs are represented in Mean ± Standard Deviation ($n = 3$)

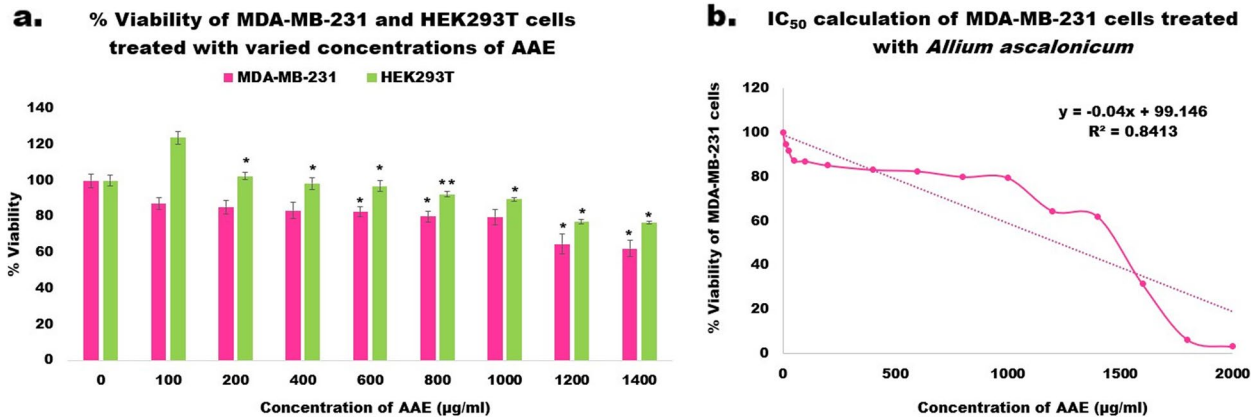

Fig. 3 **a** Cytotoxicity evaluation on MDA-MB-231 cell line to determine the percentage viability using MTT assay. **b** IC_{50} calculation of TNBC cells treated with *Allium ascalonicum* using linear line equation, $y = mx + c$, $R.^2 = 0.84$ and $IC_{50} = 1.23$ mg/ml. c. Cytotoxicity evaluation on HEK293T cell lines to determine the percentage viability using MTT assay. *$p \leq 0.05$ (statistically significant) and **$p \leq 0.005$ (high statistical significance). Error bars in the graphs represent Mean ± Standard Deviation. ($n = 3$)

compared to the TNBC cell line. Observation of the cells under phase contrast inverted microscope (Fig. 5a), clearly demonstrates that, TNBC cells treated with IC_{50} concentration of AAE, exhibited loss in the quantity of cells and its structural features greatly deviated from the normal morphology, in contrast to the HEK293T cells that exhibited a minimal reduction in the number of cells with no significant morphological change (Fig. 5a) as those observed in TNBC cell lines.

AAE reduces IC_{50} dosage of standard drug, Doxorubicin Hydrochloride in TNBC

MDA-MB-231 cells treated with Doxorubicin Hydrochloride as a standalone had an IC_{50} of 2.031 µg/ml (Fig. 4a). However, when these cells were treated with a combination of Doxorubicin Hydrochloride and IC_{50} of AAE, the IC_{50} value of the combination therapy was observed at 0.701 µg/ml + ($IC_{50} = 1.23$ mg/ml) of AAE (Fig. 4b). Hence, the dosage of the standard drug (IC_{50}) reduced by 65.5%, from 2.031 µg/ml (Doxorubicin

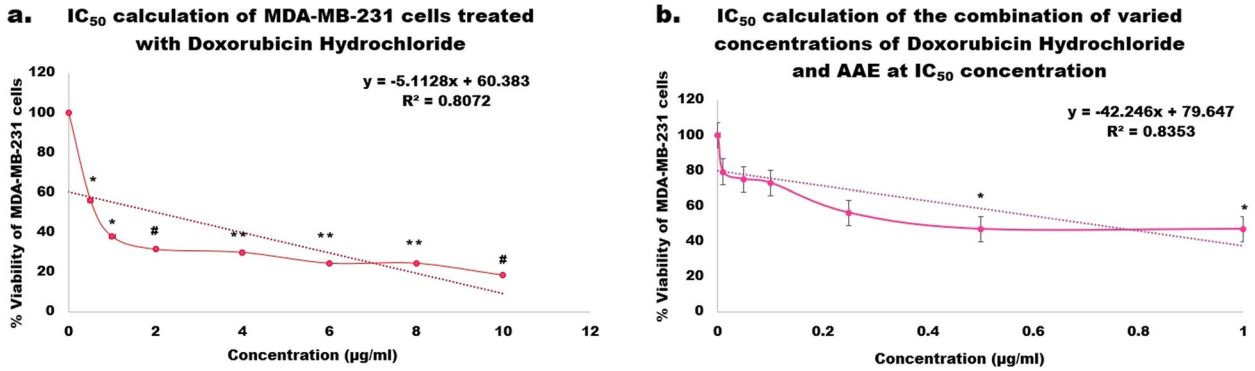

Fig. 4 **a** Cytotoxicity and IC_{50} calculation of TNBC cells treated with the standard, Doxorubicin Hydrochloride **b** Cytotoxicity and IC_{50} calculation of TNBC cells treated with varied concentrations of Doxorubicin Hydrochloride and IC_{50} concentration of AAE. *$p \leq 0.05$ (statistically significant), **$p \leq 0.005$ (high statistical significance) and # (highest statistical significance). Error bars in the graphs represent Mean ± Standard Deviation ($n = 3$)

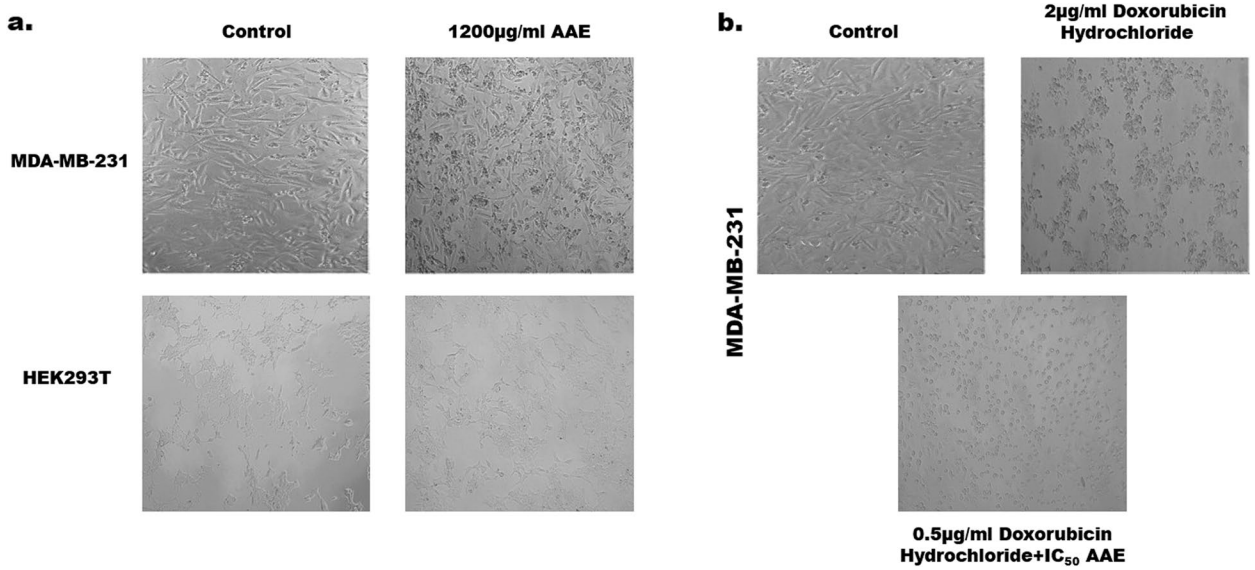

Fig. 5 **a** Microscopic observation (10X magnification) of morphological changes within MDA-MB-231 cells and HEK293T cells treated using IC_{50} concentration of AAE when compared to the control (untreated). It can be clearly observed that in AAE treated cells, MDA-MB-231 cells loses its spindle shaped morphology, transforming into more dark and circular apoptotic bodies, whereas, no significant morphological changes were observed in HEK293T cells. **b** Microscopic observation (10X magnification) of morphological changes within MDA-MB-231 cells treated with IC_{50} concentration of Doxorubicin Hydrochloride as a standalone and a combination of IC_{50} concentration of Doxorubicin Hydrochloride and AAE when compared to the control (untreated). Significant morphological changes were observed in the treated cells when compared to the untreated cells (control)

standalone treatment) to 0.701 µg/ml (combination therapy) proving the synergistic effect of the standard drug with the anti-neoplastic potential of AAE. Microscopically, a clear distinction between the control and the treated cells were also observed as represented (Fig. 5b).

AAE inhibits cell migration and clone formation

The anti-metastatic activity of AAE was determined by the ability of AAE treated (IC_{50}) MDA-MB-231 cells to migrate into the area of wound creation and also by its ability to form clones from single cell suspensions. From the microscopic images (Fig. 6a), it can be clearly observed that after 24-h treatment period of MDA-MB-231 cells with IC_{50} concentration of AAE, hardly

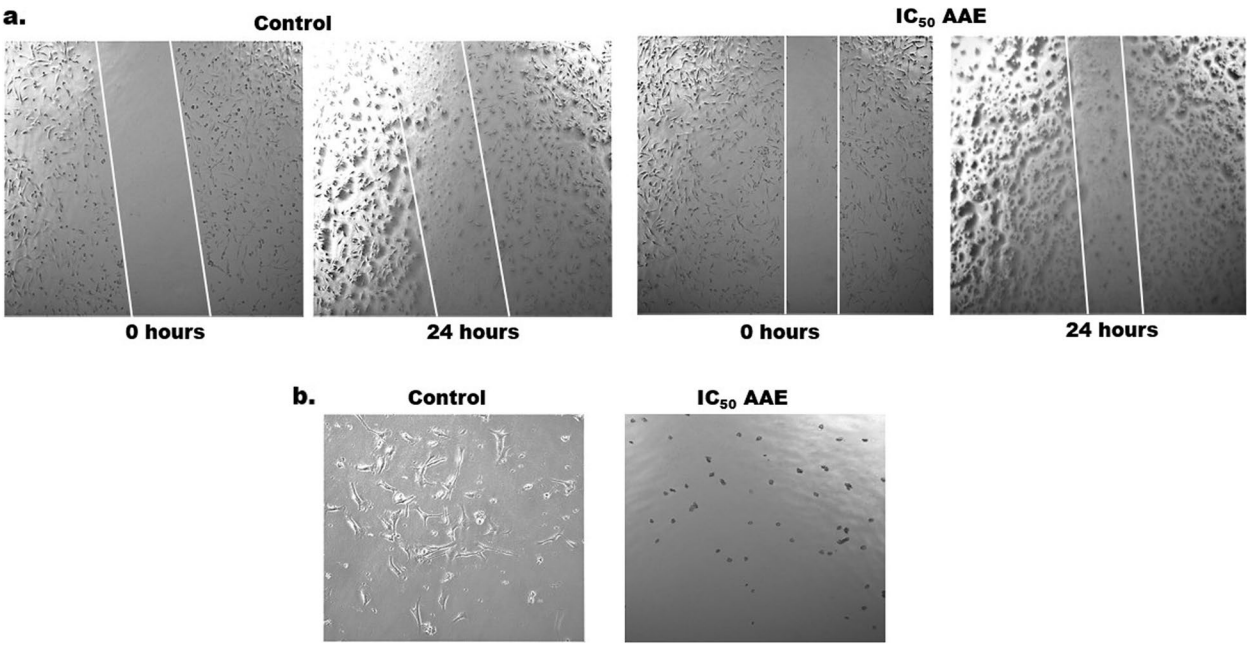

Fig. 6 **a** Cell migration Assay (10X magnification). At 0 h, the control and AAE treated cells had a clear pathway in the wounded area, whereas, after 24 h, cell migration to the wounded area was distinctly visible in the control cells, unlike the IC_{50} AAE treated cells, where only very few cells seem to have migrated in the wounded area. **b** Percentage cell migration. After 24 h of treatment period, 2.66% cell migration observed in IC_{50} AAE treated cells, unlike in Control, where 95.01% was observed. *$p \leq 0.05$ denotes statistical significance of the experiment and error bars in the graph represent Mean ± Standard Deviation ($n = 3$). c. Clonogenic Assay (10X magnification). Control cells displayed formation of clones, whereas, IC_{50} AAE treated cells, exhibited dark and circular patch of cells, confirming absence of clone formation

a few cells have migrated into the wound area, that is only about 2.66% cell migration was observed, unlike the ones observed in the untreated control cells, where, 95.01% cell migration was observed. The percentage of cell migration was determined using ImageJ analysis and represented as a graph (Fig. 6b).

Similarly (Fig. 6c), it can be visualized that clones have been formed in the control cells, whereas, in the treated ones, the TNBC cells have lost its ability to form clones and hence the picture displays cells as dark patches. Thus, it can be concluded that, MDA-MB-231 cells treated with AAE loses the metastatic property and hence has the ability to prevent the development of advanced stages of TNBC.

AAE treatment induces apoptosis and necrosis of MDA-MB-231 cells

Induction of apoptosis and necrosis by AAE on MDA-MB-231 cells can be clearly observed when both AAE treated at IC_{50} and untreated cells were stained using AO/EtBr as depicted (Fig. 7). The nucleus of the live cells does not show any condensation, whereas, the nucleus of the early apoptotic cell exhibited either granular or crescent shape and established towards one side of the cell. The nucleus of the cells at the late apoptotic stage displayed orange fluorescence generated from EtBr staining and are found to be concentrated at a specific location. The necrotic cells were found to exhibit orange fluorescence with an increased cell volume and an undefined outline due to membrane disintegration [23, 24]. Table 3, represents the percentage rate of apoptotic cells determined in the control and the IC_{50} of AAE treated group of MDA-MB-231 cells. Thus, dual AO/EtBr fluorescence staining assay confirmed that AAE has the capacity to induce apoptosis and necrosis in MDA-MB-231 cells that can be formulated suitably to treat TNBC.

Discussion

The protein targets used in our in silico study has distinct functional characteristics and each one of them play a very crucial role in the etiology of cancer. A multimeric protein complex, NLRP3 (Nucleotide-Binding Domain, Leucine-Rich–Containing Family, Pyrin Domain–Containing-3) inflammasome, gets activated in response to certain cellular disturbances leading to the pathogenesis of inflammation associated diseases, such as Cancer [26]. These in turn activate the release of inflammatory cytokines, like, IL-18, described to be overly expressed in inflammatory breast cancer [26, 27]. IL-18 was also reported to correlate positively with metastasis of lymph nodes in patients with breast neoplasms [28], making it

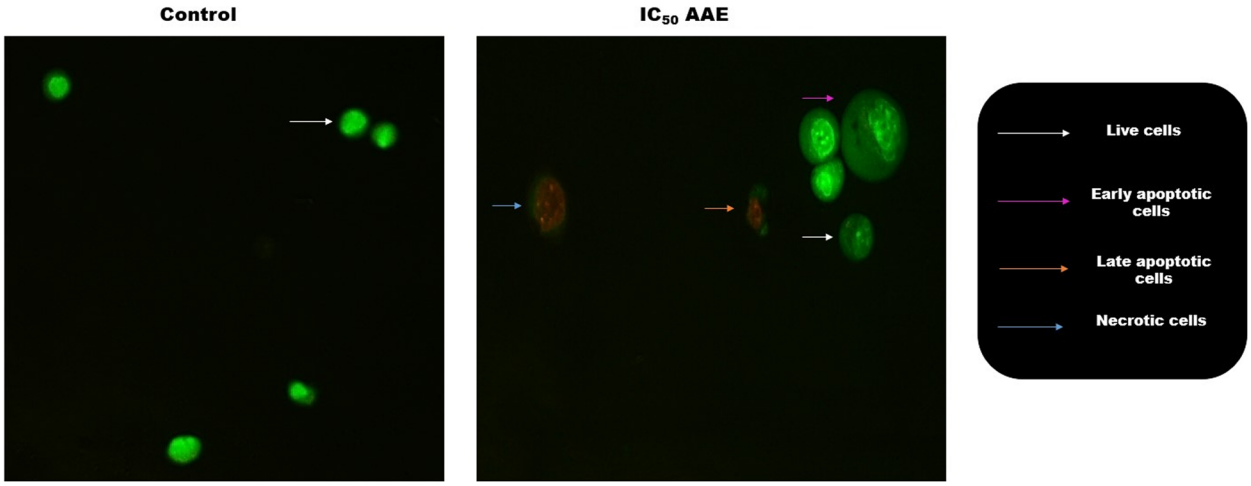

Fig. 7 Observation of MDA-MB-231 cells after Dual Acridine Orange/Ethidium Bromide (AO/EtBr) fluorescence staining. Uniform distribution of green fluorescence in live cells can be observed in control, whereas, in IC_{50} AAE treated cells, live cells, early apoptotic cells (nucleus-granular or crescent shape), late apoptotic cells (nucleus stained red and the remaining portion of the cell had stained light green) and necrotic cells (huge cell volume, orange-red coloured with undefined outer membrane implying membrane disintegration) were observed

Table 3 Percentage rate of apoptosis in the Control and IC_{50} of AAE treated MDA-MB-231 cells

Group	Types of cells	Percentage of cells (%)	Rate of apoptosis (%)
Control	Live cells	100	0
IC_{50} treated MDA-MB-231 cells	Live cells	16.67	83.34
	Early apoptotic cells	50	
	Late apoptotic cells	16.67	
	Necrotic cells	16.67	

one of the most targetable inflammatory cytokines to inhibit the progression of breast cancer malignancy.

A crucial biological process that occurs in response to cellular stress or developmental cues is apoptosis. In addition to being a major factor in the genesis of cancer, impaired apoptosis also lessens the effectiveness of conventional cytotoxic treatments. BCL-2 family of proteins, play a critical role in regulating pro- and anti-apoptotic activities, leading to subtle balance in healthy cells, however, in tumor cells, BCL-2 protein (anti-apoptotic) belonging to the sub-group of BCL-2 family, were found to be overexpressed than in normal cells. In order to enhance apoptosis of tumor cells and also to overcome the chemotherapeutic resistance, BCL-2 can be one of the significant targets for drug development [29].

MCL-1 (Myeloid Cell Leukemia-1) is another significant anti-apoptotic protein that binds to the pro-apoptotic subgroup of BCL-2 protein family to prevent apoptosis. Enhanced expression of MCL-1 has been observed in numerous tumor types and is linked with cell neoplastic transformation, defective prognosis and resistance to chemotherapeutic drugs [30]. MCL-1 was also observed to play a vital part in regulating the apoptotic pathway of mitochondria and hence it is a fascinating target for breast cancer therapy [30].

Vimentin is a type of Intermediate Filament, often found to be overly expressed in advanced neoplasms, enabling them for cell migration and invasion, leading to metastasis. It was also found to correlate with stimulating epithelial to mesenchymal cell transition (EMT pathway) and diminished patient survival, making it one of the interesting targets for advanced neoplasms of the breast [31, 32]. Hence, targeting these specific proteins involved in key cellular processes is critical for inhibiting cancer progression. Phytocompounds derived from natural sources, with the capacity to selectively target these proteins, hold significant potential for the development of novel therapeutic strategies in treating TNBC.

Scientific reports have already been established that, Isoquinoline derivatives possess moderate cytotoxic effect on Human Leukemia cell line (HL60) and Human colorectal carcinoma cell line (HCT116) and low toxicity against normal cell line, human lung fibroblast (MRC5). It also stated that benzyloxy group in the Isoquinoline, 1-[3,5-benzyloxybenzyl]−6-methoxy-N-methyl- was majorly responsible for the cytotoxic effect on cancer cell lines [33]. Furthermore, research works have suggested that succinic acid demonstrated anti-neoplastic effect on cancer cell lines by inducing apoptosis in renal cancer cell lines with no cytotoxic effect on normal cell line, MRC-5 [34]. Hence, Succinic acid, diamide, N, N′-diethyl-N, N′-diphenyl-, identified as a potential phytocompound through molecular docking studies can be a

potential option for cancer treatment. Similarly, a pyrrole derivative was found to possess good apoptotic inducing effect against three cell lines of breast carcinomas, T47-D, MCF-7 and MDA-MB-231 [35]. Another study reported that a pyrrole imidazole polyamide can be effective against cervical cancer through DNA-alkylation of tumor cells [36]. Therefore, Pyrrole, 2-methyl-5-phenyl- can serve as one of the significant treatment options for averting the progression of TNBC.

The three significant bioactive compounds, Isoquinoline, 1-[3,5-benzyloxybenzyl]−6-methoxy-N-methyl-; Succinic acid, diamide, N, N′-diethyl-N, N′-diphenyl- and Pyrrole, 2-methyl-5-phenyl- have been found to effectively interact with target proteins, implying the fact that these compounds would be playing a major role as an anti-inflammatory, cytotoxic and anti-metastatic therapeutic agent prohibiting the progression of TNBC stages.

The best phytocompound in terms of binding affinity scores among the anti-neoplastic compounds obtained through LC–MS, Rhusflavone, previously isolated from the fruit of *Rhus parviflora* demonstrated cytotoxic activity against HCT-116, MCF-7 and HeLa with IC_{50} values ranging between 17–19 μM for each of these cell lines. The puckered conformation of the C ring in the flavone with C2 and C3 carbons lying on the opposite sides of the planar A ring was found to be responsible for the significant cytotoxicity against the three cell lines [37]. Hence, from the above work, we confirm that Rhusflavone would be one the best anti-neoplastic phytocompounds in preventing the progression of TNBC. The second best phytocompound, Epigallo Catechin Gallate, known for its abundance in green tea, were reported to possess preventive activity of inflammation-derived DNA damage and carcinogenesis [38]. It has also been proved to antagonize the progression of digestive tract tumors [39]. The compound was also found to regulate and inhibit various signaling pathways, namely, EGFR, JAK-STAT, MAPKs, NF-κB, PI3K-AKT-mTOR [40] involved in the regulation of proliferation, apoptosis and angiogenesis in cancers of cervix, breast, ovary, endometrium, pancreas, gastric, liver, colon, bile duct, renal, prostrate, urinary bladder, head and neck, oral, leukemia, lymphoma, oesophagus, melanoma, lung, myeloma, osteosarcoma, brain, retina, endocrine etc. [41].

The protein complexes of the innate immune system known as inflammasomes cause inflammation in response to endogenous danger signals or externally invading microroganisms. Three proteins make up inflammasome multiprotein complex: pro-caspase-1, an adapter and a sensor protein. When the inflammasome is activated, caspase-1 is triggered resulting in cleavage of the pro-inflammatory cytokines like, IL-1β (Interleukin 1-Beta) and IL-18, causing pyroptosis. Disorders of the neurodegenerative system, cancer, certain metabolic and cardiovascular dieseases have all been linked to abnormal signaling of the inflammasome [42]. Functional abnormality of the inflammasome has also been reported to be responsible for overexpression of IL-18 in inflammatory breast cancer [27]. Hence, it has become crucial for the anti-neoplastic drugs to possess the property of anti-inflammation. Through molecular docking studies, it was already proved that phytocompounds of AAE target IL-18. Additionally, this in vitro assay validated the fact that, AAE possess anti-inflammatory property, making AAE one of the significant, non-toxic drugs that can be used for treating TNBC.

The outcomes from MTT assay, exhibited the fact, that the spindle-shaped normal TNBC cells (untreated cells-control), depicted more circular shaped apoptotic bodies on treatment with AAE. Treatment of TNBC cells with AAE proved to be more toxic than its treatment to normal human embryonic kidney cell line, validating the fact that AAE has chemotherapeutic effect only on cancer cells, sparing the normal cells and hence can serve as one of the excellent chemotherapeutic drugs with minimal toxic side-effects. Subsequently, the combination of treating TNBC cells with AAE and Doxorubicin hydrochloride (standard), reduced the dosage of the standard significantly, exhibiting synergistic effect and also reduced use of conventional drugs for treating the disease. Dual fluorescent staining of MDA-MB-231 cells using AO/EtBr also reflected the induction of apoptosis and necrosis in AAE treated cells. Additionally, molecular docking studies revealed that phytocompounds of AAE could interact with anti-apoptotic proteins, BCL-2 and MCL-1, that might probably interrupt its function, facilitating increased apoptosis of cancer cells. MTT and dual fluorescent staining assays performed in our research work, also authenticated the same findings, validating the fact that, AAE possess chemotherapeutic potential by inducing anti-proliferative and apoptosis in MDA-MB-231 cells.

In silico, molecular docking studies, identified that phytocompounds of AAE could inhibit the activity of intermediate filament, Vimentin, which would otherwise, help the cells to gain mobility, facilitating them to metastasize through EMT pathway [31, 32]. Additionally, in vitro assays, such as cell migration and clonogenic assays substantiated the molecular docking results, revealing the fact that, AAE could act as an excellent anti-neoplastic drug for TNBC.

Furthermore, in vitro assays suggested that IC_{50} concentration of AAE induces both apoptosis and inhibition of cell migration. While apoptosis and inhibition of cell migration are distinct processes, they are not mutually exclusive, and it is possible for a compound to influence both simultaneously through different mechanisms. AAE

may induce apoptosis by activating intrinsic or extrinsic apoptotic pathways, while simultaneously inhibiting cell migration by interfering with key signaling molecules or the cellular machinery involved in migration. Hence, we hypothesize that, this dual effect of AAE might be attributed to distinct co-existing mechanisms, which can further be explored in near future, through gene expression studies and in vivo animal models.

Conclusion

Our research work on understanding the anti-neoplastic potential of *Allium ascalonicum* in treating TNBC was performed through both, in silico and in vitro assays. Molecular docking results recognized three significant potential bioactive compounds obtained through GC–MS, Isoquinoline, 1-[3,5-benzyloxybenzyl]−6-methoxy-N-methyl-; Succinic acid, diamide, N, N′-diethyl-N, N′-diphenyl- and Pyrrole, 2-methyl-5-phenyl- and five significant bioactive compounds obtained through LC–MS, namely, Rhusflavone, Epigallo Catechin Gallate, Phylloquinone, Myricitrin and Obtusinin that have the ability to act as an anti-inflammatory, anti-proliferative, cytotoxic and anti-metastatic agents by targeting IL-18, BCL-2, MCL-1 and Vimentin through appropriate interactions and hence regulating its expression**.** The same results were also authenticated through relevant in vitro assays. AAE extract proved to be cytotoxic against MDA-MB-231 cells and not against HEK293T cells. In addition, TNBC cells treated with the combination of AAE extract and the standard drug, Doxorubicin Hydrochloride, reduced the IC_{50} value of the standard by 65.5% and hence averting the ill-effects of the conventional treatment. Furthermore, cell migration assay and clonogenic assay proved that AAE suppresses cell migration and clone formation, proving its therapeutic potential at the metastatic stage of TNBC. On a broader perspective, animal model experiments and consequently pre-clinical and clinical trials would be required to confirm the efficacy of the anti-neoplastic bioactive compounds of *Allium ascalonicum,* so that, they can be standardized as an appropriate formulation for the treatment of Triple-Negative Breast Cancer. It can also be said that, Shallots, one of the commonly used ingredients in various cuisines throughout the world, has the capability to provide us the essential nutrition to combat TNBC when consumed on a regular basis, proving its worth.

Abbreviations

AAE	Aqueous *Alliumascalonicum* extract
GC-MS	Gas Chromatography-Mass Spectrometry
LC-MS	Liquid Chromatography-Mass Spectrometry
IL-18	Interleukin-18
BCL-2	B-cell Lymphoma-2
MCL-1	Myeloid Cell Leukemia-1
BSA	Bovine Serum Albumin
TNBC	Triple-Negative Breast Cancer
MTT	3-(4,5-Dimethylthiazol-2-yl)-2,5-Diphenyltetrazolium Bromide
MDA-MB-231	MD Anderson-Metastatic Breast-231 Cells
HEK293T	Human embryonic kidney 293 T cells
AO/EtBr	Acridine Orange/Ethidium Bromide
BRCA1	Breast Cancer gene 1
HER2	Human Epidermal Growth Factor Receptor 2
NLRP3	Nucleotide-Binding Domain, Leucine-Rich–Containing Family, Pyrin Domain–Containing-3
PDB	Protein Data Bank
ADME	Absorption, Distribution, Metabolism and Excretion
TBS	Tris-Buffered Saline
DMEM	Dulbecco's Modified Eagle Medium
DMSO	Dimethyl Sulfoxide
IC_{50}	Half-maximal inhibitory concentration

Supplementary Information

The online version contains supplementary material available at https://doi.org/10.1186/s12885-025-13796-8.

Additional file 1

Acknowledgements

The authors are very much grateful to the School of Life Sciences, B. S. Abdur Rahman Crescent Institute of Science and Technology, Chennai, for providing research facilities and also for their unconditional support and encouragement.

Authors' contributions

"HS conceived the idea, and supervised the research. KJR performed the experiments and analyzed the data. Both the authors wrote the manuscript and agreed to submit the current version."

Funding

This work was supported by University Grants Commission (UGC), Scheme No. 18, SJSGC 2022–23, New Delhi, India [UGC Award letter Number: F. No. 82–7/2022(SA-III) and UGC-Reference Number: UGCES-22-OB-TAM-F-SJSGC-6471].

Data availability

"Data will be made available from corresponding author on reasonable request."

Declarations

Ethics approval and consent to participate

Not applicable, as human subjects and verterbrate animals were not used in this study and hence clinical trial number is not applicable.

Consent for publication

Not applicable.

Competing interests

The authors declare no competing interests.

Author details

[1]School of Life Sciences, B. S. Abdur Rahman Crescent Institute of Science & Technology, Vandalur, Chennai 600048, India.

Received: 4 November 2024 Accepted: 24 February 2025
Published online: 07 March 2025

References

1. Van Den Ende NS, Nguyen AH, Jager A, Kok M, Debets R, Van Deurzen C. Triple-Negative Breast Cancer and Predictive Markers of Response to Neoadjuvant Chemotherapy: A Systematic Review. Int J Mol Sci. 2023;24(3):2969. https://doi.org/10.3390/ijms24032969.

2. Lehmann BD, Bauer JA, Chen X, Sanders ME, Chakravarthy AB, Shyr Y, Pietenpol JA. Identification of human triple-negative breast cancer subtypes and preclinical models for selection of targeted therapies. J Clin Invest. 2011;121(7):2750–2767. https://doi.org/10.1172/JCI45014.
3. Prat A, Pineda E, Adamo B, Galván P, Fernández A, Gaba L, Diez M, Viladot M, Arance A, Munoz M, et al. Clinical implications of the intrinsic molecular subtypes of breast cancer. Breast. 2015;24(Suppl 2):S26–35. https://doi.org/10.1016/j.breast.2015.07.008.
4. American Cancer Society. Triple-negative Breast Cancer. 2023 March 1 [accessed 2024 April 17] https://www.cancer.org/cancer/types/breast-cancer/about/types-of-breast-cancer/triple-negative.html.
5. Borri F, Granaglia A. Pathology of triple negative breast cancer. Semin Cancer Biol. 2021;72:136–45. https://doi.org/10.1016/j.semcancer.2020.06.005.
6. Pareja F, Geyer FC, Marchiò C, Burke KA, Weigelt B, Reis-Filho J. Triple-negative breast cancer: the importance of molecular and histologic subtyping, and recognition of low-grade variants. NPJ Breast Cancer. 2016;2:16036. https://doi.org/10.1038/npjbcancer.2016.36.
7. Vashi R, Patel BM, Goyal RK. Keeping abreast about ashwagandha in breast cancer. J Ethnopharmacol. 2021;269: 113759. https://doi.org/10.1016/j.jep.2020.113759.
8. Gaillard S, Stearns V. Aromatase inhibitor-associated bone and musculoskeletal effects: new evidence defining etiology and strategies for management. Breast Cancer Res. 2011;13(2):205. https://doi.org/10.1186/bcr2818.
9. Kayl AE, Meyers CA. Side-effects of chemotherapy and quality of life in ovarian and breast cancer patients. Curr Opin Obs Gynecol. 2006;18(1):24–8. https://doi.org/10.1097/01.gco.0000192996.20040.24.
10. Sharma N, Purkayastha A. Impact of Radiotherapy on Psychological, Financial, and Sexual Aspects in Postmastectomy Carcinoma Breast Patients: A Prospective Study and Management. Asia Pac J Oncol Nurs. 2017;4(1):69–76. https://doi.org/10.4103/2347-5625.199075.
11. Morris CA, Avorn J. Internet marketing of herbal products. JAMA. 2003;290(11):1505–9. https://doi.org/10.1001/jama.290.11.1505.
12. Moldovan C, Frumuzachi O, Babotă M, Barros L, Mocan A, Carradori S, Crisan G. Therapeutic Uses and Pharmacological Properties of Shallot (*Allium ascalonicum*): A Systematic Review. Front Nutr. 2022;9:903686. https://doi.org/3389/fnut.2022.903686.
13. Pandurangan V, Amanulla SSD, Ramanathan K. Anticancer efficacy of dry and fresh *Allium ascalonicum* (shallot) against HepG2 cell line. Natl J Physiol Pharm Pharmacol. 2016;6(3):196–9. https://doi.org/10.5455/njppp.2016.6.08012016112.
14. Mohammadi-Motlagh HR, Mostafaie A, Mansouri K. Anticancer and anti-inflammatory activities of shallot (*Allium ascalonicum*) extract. Arch Med Sci. 2011;7(1):38–44. https://doi.org/10.5114/aoms.2011.20602.
15. Ravindranath KJ, Christian SD, Srinivasan H. Screening of Anti-carcinogenic Properties of Phytocompounds from Allium ascalonicum for Treating Breast Cancer Through In Silico and In Vitro Approaches. Appl Biochem Biotechnol. 2023;195(2):1136–57. https://doi.org/10.1007/s12010-022-04202-1.
16. Mir MA, Bashir N, Alfaify A, Oteef M. GC-MS analysis of *Myrtus communis* extract and its antibacterial activity against Gram-positive bacteria. BMC Complementary Medicine and Therapies. 2020;20(1):86. https://doi.org/10.1186/s12906-020-2863-3.
17. Kaur J, Dhiman V, Bhadada S, Katare OP, Ghosal G. LC/MS guided identification of metabolites of different extracts of Cissus quadrangularis. Food Chemistry Advances. 2022;1: 100084. https://doi.org/10.1016/j.focha.2022.100084.
18. Trott O, Olson AJ. AutoDock Vina: improving the speed and accuracy of docking with a new scoring function, efficient optimization, and multithreading. J Comput Chem. 2010;31(2):455–61. https://doi.org/10.1002/jcc.21334.
19. Kola P, Metowogo K, Manjula SN, Katawa G, Elkhenany H, Mruthunjaya KM, Eklu-Gadegbeku K, Aklikokou KA. Ethnopharmacological evaluation of antioxidant, anti-angiogenic, and anti-inflammatory activity of some traditional medicinal plants used for treatment of cancer in Togo/Africa. J Ethnopharmacol. 2022;283:114673. https://doi.org/1016/j.jep.2021.114673.
20. Park HS, Choi EJ, Lee J-H, Kim G-H. Evaluation of *Allium* vegetables for Anti-Adipogenic, Anti-Cancer, and Anti-Inflammatory Activities *In Vitro*. J Life Sci. 2013;5(2):127–32. https://doi.org/10.1080/09751270.2013.11885219.
21. Rafehi H, Orlowski C, Georgiadis GT, Ververis K, El-Osta A, Karagiannis TC. Clonogenic Assay: Adherent Cells JoVE. 2011;49:2573. https://doi.org/10.3791/2573.
22. Begum SMFM, Chitra K, Joseph B, Sundararajan R, Srinivasan H. Gelidiella acerosa inhibits lung cancer proliferation. BMC Complement Altern Med. 2018;18:104. https://doi.org/1186/s12906-018-2165-1.
23. Liu K, Liu PC, Liu R, Wu X. Dual AO/EB staining to detect apoptosis in osteosarcoma cells compared with flow cytometry. Med Sci Monit Basic Res. 2015;21:15–20. https://doi.org/10.12659/MSMBR.893327.
24. Kepekçi AH, Gündoğan Gİ, Kig C. In Vitro Physiological Effects of Betahistine on Cell Lines of Various Origins. Turk J Pharm Sci. 2021;18(2):140–5. https://doi.org/10.4274/tjps.galenos.2020.88155.
25. Cancer Research UK. Gemcitabine (Gemzar). 2021 December 28 [accessed 2024 April 10] https://www.cancerresearchuk.org/about-cancer/treatment/drugs/gemcitabine.
26. Sharma BR, Kanneganti TD. NLRP3 inflammasome in cancer and metabolic diseases. Nat Immunol. 2021;22(5):550–9. https://doi.org/10.1038/s41590-021-00886-5.
27. Aguiar MAN, Wanderley CWS, Nobre LMS, Alencar MRM, Saldanha MDPS, Souza AM, Wong DVT, Barros PG, Almedia PRC, Lima-Junior RCP, et al. Interleukin-18 (IL-18) is equally expressed in inflammatory breast cancer and noninflammatory locally advanced breast cancer: A possible association with chemotherapy response. Asia Pac J Clin Oncol. 2018;14(2):e138–44. https://doi.org/10.1111/ajco.12722.
28. Ma T, Kong M. Interleukin-18 and -10 may be associated with lymph node metastasis in breast cancer. Oncol Lett. 2021;21(4):253. https://doi.org/10.3892/ol.2021.12515.
29. Qian S, Wei Z, Yang W, Huang J, Yang Y, Wang J. The role of BCL-2 family proteins in regulating apoptosis and cancer therapy. Front Oncol. 2022;12: 985363. https://doi.org/10.3389/fonc.2022.985363.
30. Wang H, Guo M, Wei H, Chen Y. Targeting MCL-1 in cancer: current status and perspectives. J Hematol Oncol. 2021;14(1):67. https://doi.org/1186/s13045-021-01079-1.
31. Strouhalova K, Přechová M, Gandalovičová A, Brábek J, Gregor M, Rosel D. Vimentin Intermediate Filaments as Potential Target for Cancer Treatment. Cancers (Basel). 2020;12(1):184. https://doi.org/10.3390/cancers12010184.
32. Thaiparambil JT, Bender L, Ganesh T, Kline E, Patel P, Liu Y, Tighiouart M, Vertino PM, Harvey D, Garcia A, et al. Withaferin A inhibits breast cancer invasion and metastasis at sub-cytotoxic doses by inducing vimentin disassembly and serine 56 phosphorylation. Int J Cancer. 2011;129(11):2744–55. https://doi.org/10.1002/ijc.25938.
33. Costa EV, Soares LDN, Chaar JDS, Silva VR, Santos LS, Koolen HHF, Da Silva FMA, Tavares JF, Zengin G, Soares MBP, et al. Benzylated Dihydroflavones and Isoquinoline-Derived Alkaloids from the Bark of *Diclinanona calycina* (Annonaceae) and Their Cytotoxicities. Molecules. 2021;26(12):3714. https://doi.org/10.3390/molecules26123714.
34. Kasarci G, Ertugrul B, Iplik ES, Cakmakoglu B. The apoptotic efficacy of succinic acid on renal cancer cell lines. Med Oncol. 2021;38(12):144. https://doi.org/1007/s12032-021-01577-9.
35. Moghadam ES, Amini M. 2-[2-Methyl-5-phenyl-1-(3,4,5-trimethoxyphenyl)-1H-pyrrol-3-yl]-2-oxo-N-(pyridin-4-yl) acetamide. Molbank. 2018;3:1002. https://doi.org/10.3390/M1002.
36. Krishnamurthy S, Yoda H, Hiraoka K, Inoue T, Lin J, Shinozaki Y, Watanabe T, Koshikawa N, Takatori A, Nagase H. Targeting the mutant PIK3CA gene by DNA-alkylating pyrrole-imidazole polyamide in cervical cancer. Cancer Sci. 2021;112(3):1141–9. https://doi.org/10.1111/cas.14785.
37. Shrestha S, Park JH, Lee DY, Cho JG, Seo WD, Kang HC, Yoo KH, Chung IS, Joen YJ, Yeon SW, Baek NI. Cytotoxic and neuroprotective biflavonoids from the fruit of R*hus parviflora*. J Korean Soc Appl Biol Chem. 2012;55:557–62. https://doi.org/10.1007/s13765-012-2090-9.
38. Kawai Y, Matsui Y, Kondo H, Morinaga H, Uchida K, Miyoshi N, Nakamura Y, Osawa T. Galloylated Catechins as Potent Inhibitors of Hypochlorous Acid-induced DNA Damage. Chem Res Toxicol. 2008;21(7):1407–14. https://doi.org/10.1021/tx800069e.
39. Liu C, Li P, Qu Z, Xiong W, Liu A, Zhang S. Advances in the Antagonism of Epigallocatechin-3-gallate in the Treatment of Digestive Tract Tumors. Molecules. 2019;24(9):1726. https://doi.org/10.3390/molecules24091726.
40. Kciuk M, Alam M, Ali N, Rashid S, Głowacka P, Sundaraj R, Celik I, Yahya EB, Dubey A, Zerroug E, Kontek R. Epigallocatechin-3-Gallate Therapeutic Potential in Cancer: Mechanism of Action and Clinical Implications.

Molecules. 2023;28(13):5246. https://doi.org/10.3390/molecules28135246.
41. Almatroodi SA, Almatroudi A, Khan AA, Alhumaydhi FA, Alsahli MA, Rahmani AH. Potential Therapeutic Targets of Epigallocatechin Gallate (EGCG), the Most Abundant Catechin in Green Tea, and Its Role in the Therapy of Various Types of Cancer. Molecules. 2020;25(14):3146. https://doi.org/10.3390/molecules25143146.
42. Li Y, Huang H, Liu B, Zhang Y, Pan X, Yu XY, Shen Z, Song YH. Inflammasomes as therapeutic targets in human diseases. Signal Transduct Target Ther. 2021;6(1):247. https://doi.org/10.1038/s41392-021-00650-z.

Publisher's Note